

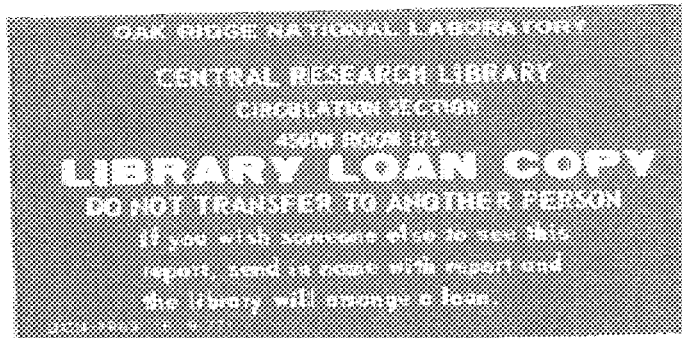
ornl

OAK RIDGE
NATIONAL
LABORATORY

MARTIN MARIETTA

Experimental and Thermodynamic
Study of Nonstoichiometry
in $\langle \text{YBa}_2\text{Cu}_3\text{O}_{7-x} \rangle$

T. B. Lindemer
J. F. Hunley
J. E. Gates
A. L. Sutton, Jr.
J. Brynestad
C. R. Hubbard
P. K. Gallagher



OPERATED BY
MARTIN MARIETTA ENERGY SYSTEMS, INC.
FOR THE UNITED STATES
DEPARTMENT OF ENERGY

Prepared under contract by Battelle Seattle Research Center
Austrian Institute of Technology
U.S. Department of Defense
5285 Port Royal Road, Springfield, Virginia 22161
NTIS price codes--Printed Copy, \$7.25; Microfiche, \$1.75

This report was prepared as an account of work sponsored by the Defense Intelligence Agency, United States Government. Neither the United States Government nor its contractors, employees, or agents, nor any of their employees, makes any representation, warranty, or guarantee, expressed or implied, as to the usefulness of any information, apparatus, product, process, or material contained herein. The Defense Intelligence Agency represents that its use is not subject to infringement claims against the United States Government relating to any specific commercial product, process, or material. The Defense Intelligence Agency does not represent, warrant, or guarantee, expressed or implied, that the use of any apparatus, product, process, or material contained herein will not infringe upon privately owned rights. The Defense Intelligence Agency does not represent, warrant, or guarantee, expressed or implied, that the use of any apparatus, product, process, or material contained herein will not infringe upon privately owned rights.

Chemical Technology Division

EXPERIMENTAL AND THERMODYNAMIC STUDY OF NONSTOICHIOMETRY IN
 $\langle \text{YBa}_2\text{Cu}_3\text{O}_{7-\text{x}} \rangle$

T. B. Lindemer^{*}
J. F. Hunley^{**}
J. E. Gates^{**}
A. L. Sutton, Jr.
J. Brynestad[†]
C. R. Hubbard^{††}
P. K. Gallagher[‡]

^{*}Co-op student from Tennessee Technological University, Cookeville.

^{**}Co-op student from University of Tennessee, Knoxville.

[†]Chemistry Division.

^{††}Metals and Ceramics Division.

[‡]AT&T Bell Laboratories, 600 Mountain Avenue, Murray Hill, NJ 07974.

Date Published: May 1989

Submitted for publication to the Journal of the American Ceramic Society.

Prepared for the
Division of Materials Sciences, Office of Basic Energy Sciences
KC 02 03 02 0

Prepared by the
OAK RIDGE NATIONAL LABORATORY
Oak Ridge, Tennessee 37831-6285
operated by
MARTIN MARIETTA ENERGY SYSTEMS, INC.
for the
U.S. DEPARTMENT OF ENERGY
under contract DE-AC05-84OR21400



3 4456 0298829 3

CONTENTS

ABSTRACT	1
1. INTRODUCTION	1
2. SYNOPSIS OF PREVIOUS STUDIES	2
3. EXPERIMENTAL	5
3.1 MATERIALS	5
3.2 TGA SYSTEM AND PROCEDURE	6
3.3 HYDROGEN REDUCTION	7
3.4 O/6M VALUES FOR "123"	9
3.5 DECOMPOSITION OF "123"	15
3.6 REACTION OF "123" WITH (CO ₂) + (O ₂)	15
4. CHEMICAL THERMODYNAMIC REPRESENTATIONS	15
5. GENERAL DISCUSSION	20
5.1 SUMMARY OF THE x-T-p _{O₂} * DATA	20
5.2 OXYGEN POTENTIALS IN THE Y-Ba-Cu-O SYSTEM	21
5.3 EQUILIBRIA WITH (CO ₂) AND (H ₂ O)	25
6. REFERENCES	27

EXPERIMENTAL AND THERMODYNAMIC STUDY OF NONSTOICHIOMETRY IN
 $\langle \text{YBa}_2\text{Cu}_3\text{O}_{7-\text{x}} \rangle$

T. B. Lindemer, J. F. Hunley, J. E. Gates, A. L. Sutton, Jr.,
J. Brynestad, C. R. Hubbard, and P. K. Gallagher

ABSTRACT

The dependence of the nonstoichiometry of $\langle \text{YBa}_2\text{Cu}_3\text{O}_{7-\text{x}} \rangle^*$ has been studied over five orders of magnitude in oxygen pressure and from 573 to 1173 K. These data were used to derive a chemical thermodynamic representation that correlates the experimental variables. The data were also compared with several other investigations to identify the self-consistent sets of data. Hydrogen-reduction methods for determining the absolute oxygen-to-metal ratio were developed. The effects of carbonate and hydroxide equilibria were also investigated briefly.

1. INTRODUCTION

There are discrepancies in the literature data for the temperature and oxygen pressure dependence of the nonstoichiometry of $\langle \text{YBa}_2\text{Cu}_3\text{O}_{7-\text{x}} \rangle$, called "123," which is one of the recently discovered superconducting oxides. Also, there is no reported expression relating the interdependence of these experimental variables.

There are three primary objectives in this paper. First, data extracted from the literature will be reviewed to demonstrate the extent of the discrepancies. Second, we will present an extensive experimental determination of the nonstoichiometry over the ranges $573 < T < 1173$ K and $10^{-5} < p_{\text{O}_2}^* < 1.0$. ($p_{\text{O}_2}^*$ is the oxygen pressure in MPa divided by the standard-state pressure, 0.101 MPa.) Third, chemical thermodynamic representations will be derived to relate the interdependence of T, x, and the chemical potential of oxygen, $RT \ln(p_{\text{O}_2}^*)$ or oxygen potential, in which R is the gas constant, $8.314 \text{ J} \cdot \text{mol}^{-1} \cdot \text{K}^{-1}$, and T is temperature in Kelvins.

*These symbols, $\langle \rangle$, $\{ \}$, and $()$ are used to indicate a solid, liquid, and gas, respectively.

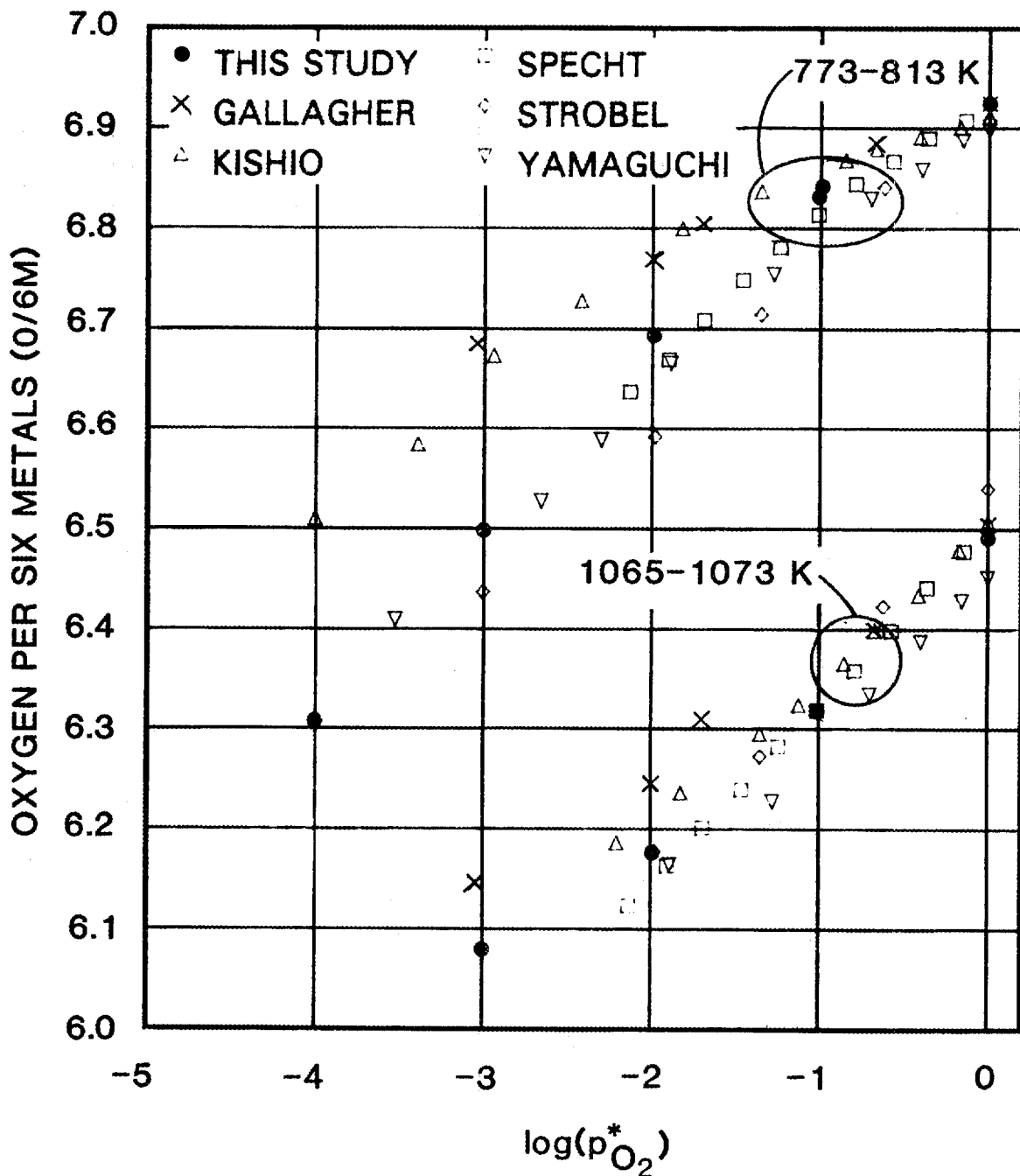
2. SYNOPSIS OF PREVIOUS STUDIES

Several thermogravimetric analyses (TGA) have been made of the dependence of oxygen per six metals (O/6M) on temperature and oxygen partial pressure. The first authors of extensive studies are Gallagher,¹ Kishio,² Specht,³ Strobel,⁴ and Yamaguchi.⁵ In addition, Takayama-Muromachi's second article^{6,7} gives limited data. These investigations have been summarized in a previous report⁸ that includes a numerical data base for each of the investigations. Very recent work has been reported at 973 to 1073 K by Tetenbaum et al.⁹ Additional investigations by Marucco et al.¹⁰ and Iwase et al.¹¹ appear so different from the others that their results were not considered further.

Some of the literature data are compared in Figs. 1 and 2. The O/6M values near 773 K and 1073 K are plotted in Fig. 1 vs $\log(p_{O_2}^*)$, while in Fig. 2, data at $p_{O_2}^* = 1, 0.01$, and 0.0001 are plotted. [Figure 2 is a convenient way to plot data and fits of data because it illustrates the Henrian linear behavior as O/6M approaches the lower limit of 6 and the upper limit of 7. The abscissa for this figure results from $m_1=m_2=2$, Eqs. (3) and (4), which are developed later.] These plots clearly demonstrate the discrepancies in the data, which will be considered in detail in the discussion section. However, it is immediately apparent from the figures that the data disagree more as $p_{O_2}^*$ is lowered, particularly at low temperatures, which suggests that equilibrium may be more difficult to establish at these conditions. The experimental details of the previous investigations were summarized in our earlier report.⁸ However, there were no apparent factors correlating the experimental methods with the disparities in the data.

Several investigations reported the maximum O/6M value. Gallagher et al.¹² determined this ratio by reduction in ($N_2-15\% H_2$) to a maximum temperature of 1273 K and obtained a maximum O/6M of 6.98 ± 0.01 . The reduced material contained only baria, yttria, and copper; they also noted retention of water, probably as hydroxides, at reduction temperatures below 1200 K. Kishio et al.² using iodometric titration, obtained a maximum O/6M of 6.93 ± 0.02 . Their maximum values seem markedly lower

ORNL DWG 88-14949



ORNL DWG 88-14951

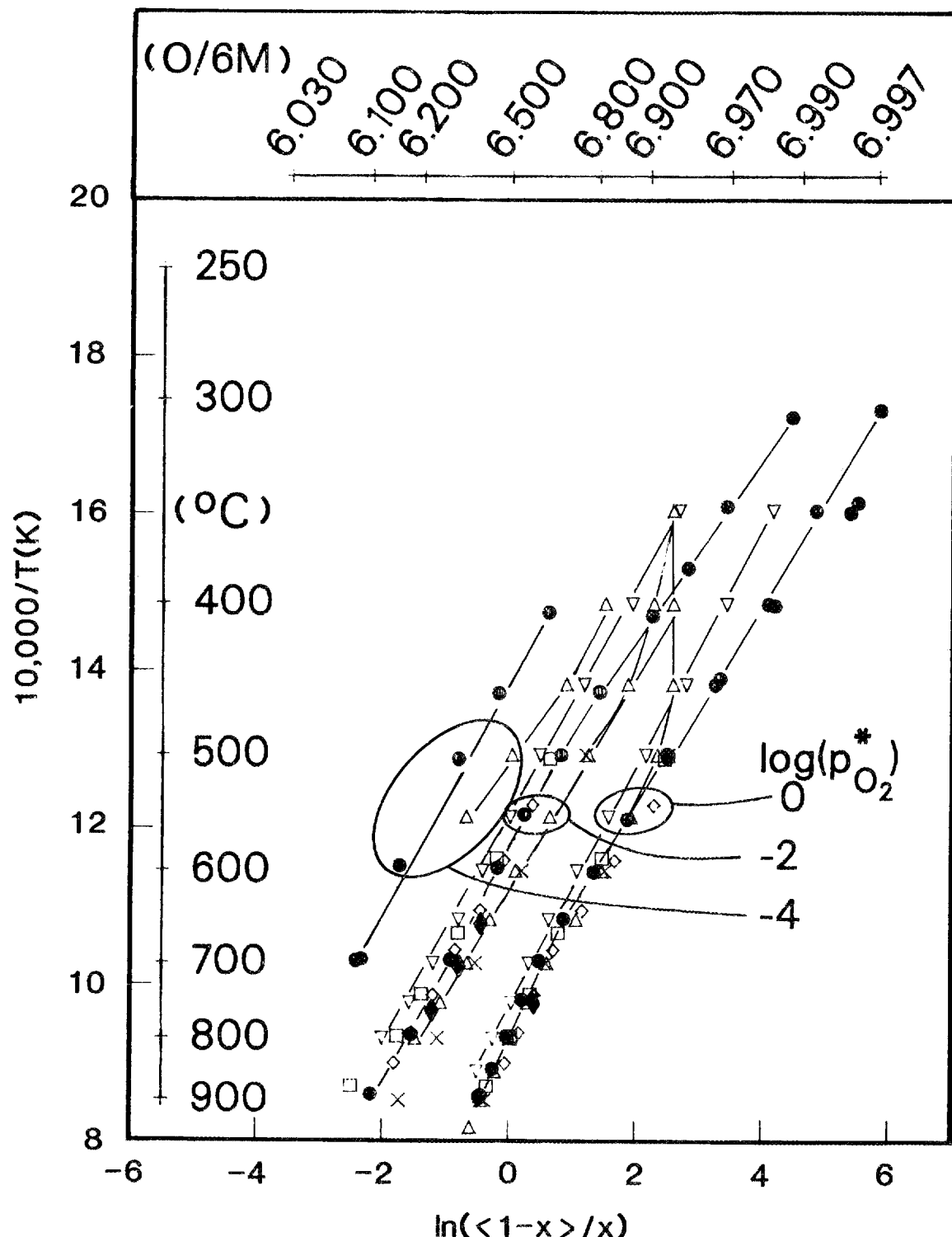


Fig. 2. Comparison of several investigations of the dependence of nonstoichiometry in the "123" compound on temperature at $p_{O_2}^*$ values of 1, 0.01, and 0.0001. The investigators are represented by the same symbols used in Fig. 1. In addition, the symbol ♦ at 923 to 1023 K represents data from ref. 9.

than those from all other investigations. Specht et al.³ using reduction in pure hydrogen at 923 K, assuming baria, yttria, and copper as final products, and a sample cooled slowly in 1 atm oxygen obtained $O/6M = 6.97 \pm 0.02$. Strobel et al.⁴ reported a maximum $O/6M$ of 7 from neutron diffraction, which was also used to indicate a single-phase material. Takayama-Muromachi et al.^{6,7} estimated the maximum $O/6M$ to be 7.0 based on hydrogen reduction at 1173 K; reduction at 923 K led to water retention, with barium hydroxide being suggested. Inert gas fusion gave 6.7, while an unspecified analysis gave 6.89. Yamaguchi et al.⁵ used a pellet that was slowly cooled to ambient in oxygen, then reduced at 2973 K, giving an $O/6M$ of 6.95 to 7.01. They subsequently assumed that treatment at 473 K in oxygen gave 7.00, which was consistent with their observation of $\log(x)$ vs $\log(p_0^*/p_2)$ being linear at low x (see their Fig. 2).

3. EXPERIMENTAL

3.1. MATERIALS

Several different sources of "123" materials were used. One of the authors (PKG) provided 3 g of powder, which was part of a 100-g batch, R4784-F25, made from yttria, CuO, and barium carbonate. Another author (JB) provided "123" powders made from these same materials. He also made the specimens used by Specht et al.³ All powders and subsequent pellets were protected from moisture by storage in sealed bottles containing Drierite (the dessicant calcium sulphate) and Ascarite (finely distributed NaOH to combine with carbon dioxide).

Pellets were made from these materials and were used for the TGA studies. About 1 to 2 g of powder was ground in an alumina mortar and pestle under toluene until no grittiness was felt. The toluene protects the material from interaction with laboratory air and moisture and dissolves <0.5 mg/L quantities of "123."¹³ Examination of this powder in the scanning electron microscope demonstrated a particle size of <5 μm . The toluene was evaporated to remove most of the liquid, the powder was pressed very lightly into a 1-cm-diam pellet, additional toluene evaporated in flowing nitrogen in a quartz tube furnace at 373 K, and then the

pellet was finally heated to 1173 K in flowing oxygen for a few hours. The entrant gases were first passed through Ascarite and Drierite to remove water and carbon dioxide. This procedure gave an ~0.8-cm-diam, ~1.0-cm-long pellet of about 65% of theoretical density. This pellet was used in the TGA for a series of studies, then sliced under toluene into ~0.8-cm-diam, ~0.1-cm-thick discs to give a final data set.

Pellets for ceramography were made from about 150 mg of the powder that was pressed into a right circular cylinder at about 30,000 psi (207 MPa) and heat treated as above to give about 90% of theoretical density.

3.2. TGA SYSTEM AND PROCEDURE

A Cahn 1000 balance was part of the TGA system that was used previously for an extensive study of nonstoichiometry in the urania-gadolinia system.¹⁴ The Cahn readout of weight change was calibrated and it was heavy by 0.3%, thus the data were corrected for this change. The true specimen temperature was determined during several calibrations that employed both optical pyrometry and thermocouples.

A commercial oxygen meter containing a stabilized-zirconia cell was used as the primary indication of oxygen partial pressure in the TGA. The meter reading was compared to gases mixed by calibrated flow meters and found to be reliable without correction. A total gas flow rate of 0.4 L/min (STP) was used and the gas was passed through Ascarite and Drierite immediately before entering the TGA furnace. The oxygen partial pressure was measured in both the furnace inlet and outlet gasses and always agreed within <0.02 log units. Data were taken at $\log_{10}(p_0^*)$ values at approximately 0, -1, -2, -3, -4, and -5. This permitted ease of visual comparison of the data with the fitted behavior (as shown in Fig. 3) during data analysis.

A typical run began by placing the 1- to 2-g pellet in a 1.8-g alumina holder suspended from the Cahn balance on a platinum wire in the center of the furnace. The Cahn unit works on a null weight basis, and the weight in mg (within about ± 0.01 mg, which is equivalent to $0/6M = \pm 0.0003$) to

ORNL DWG 88-14950

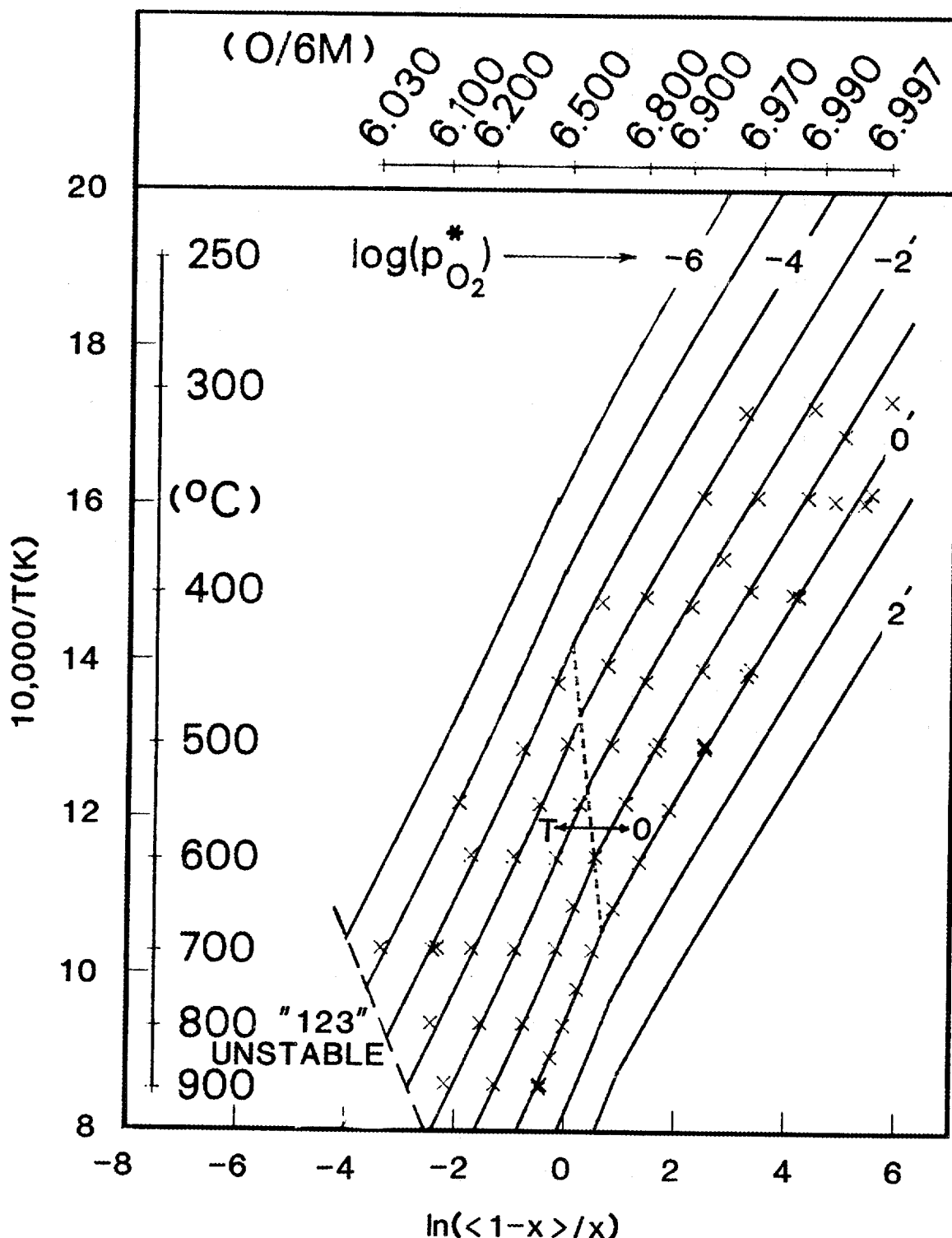


Fig. 3. The data of Table 1 and the fit of the data (lines) calculated from Eq. (9). The orthorhombic-to-tetragonal transition ($0 \approx T$, dashed line) is from Specht et al.³

null the specimen at zero gas flow was recorded on a 25-cm-wide chart recorder. For convenience, the null condition was defined as the weight needed to bring the recorder pen to mid-chart when the Cahn was configured to give one mg full scale on the chart. The specimen temperature was taken to 1173 K in oxygen to remove any residual carbonates, hydroxides, etc., that may have been introduced during handling. It was left at this temperature until the specimen equilibrated, and the zero flow weight (ZFW) noted. The specimen temperature was then taken to 773 K, equilibrated in oxygen, and the ZFW recorded; the latter became the standard reference ZFW and all specimen weight changes at other conditions were calculated relative to it. From time to time the specimen was returned to the standard reference ZFW condition, thus ensuring that any experimental condition leading to long-term drift in the reference ZFW was noted and adjusted accordingly.

Buoyancy effects were determined and were essentially equivalent to those calculated from the ideal gas law. The present data were corrected for buoyancy, although the effect is small. For example, with a 1.8-g CuO sample heated in pure oxygen, the weight change was equivalent to an O/Cu change of 0.0003 as temperature was varied from 1166 to 571 K. Without the buoyancy correction, the O/Cu would have changed by -0.0005 from 1166 to 571 K.

3.3 HYDROGEN REDUCTION

Absolute oxygen-to-metal ratios were determined in "123" and other oxides by hydrogen reductions. This procedure provided reference O/M values for "123" that could be compared with others determined from the data analyses to be presented later. Here, argon containing 4% hydrogen (Ar-4% H₂) was used in the TGA to determine the amount of oxygen removed at a given temperature during the reduction of oxide that had been equilibrated in pure oxygen at the same temperature. The results permitted calculation of the oxygen-to-metal ratios in several materials. Experience revealed that reductions of baria-containing materials at 1163 K removed all the reduction product water, while reductions at lower temperatures increased the possibility that some water might be retained (probably as

barium hydroxide) particularly at temperatures below 1073 K. Similar observations were noted by Gallagher et al.^{12,15} and Takayama-Muromachi et al.^{6,7} Since Ba(OH)₂ melts at 681 K, liquid Ba(OH)₂-based solutions may be a possibility, and they may require higher temperatures for complete water removal.

The basic procedure started with equilibration of 0.3 to 1 g of either loose or pelletized oxide powder in an oxygen flow of 0.4 L/min at 1163 K. The ZFW at 1163 K was noted, the TGA was flushed with nitrogen, and then 0.4 L/min of (Ar-4% H₂) was used for the reduction. Complete reduction was assumed upon no further loss of weight, and the second ZFW was recorded. The difference between the two ZFW values was the oxygen lost during reduction. The sample was cooled to room temperature in the TGA in flowing nitrogen, a process that required 4 h, during which the sample was partially reoxidized by about a milligram of tramp oxygen. In order to get the true weight of the reduced sample, a second reduction in flowing (Ar-4% H₂) was carried out in a quartz muffle at 1163 K. The muffle and sample were then removed from the furnace, which quenched the sample to room temperature in about 10 min, and resulted in a fully reduced sample at room temperature. The O/6M of the sample at 1163 K was then calculated from the oxygen lost during reduction in the TGA and by assuming that the fully reduced sample consisted of yttria, elemental copper, and baria, with the Y/Ba/Cu value known from the initial composition of the "123."

Reductions were performed on <CuO>, <Y₂BaCuO₅>, and <BaCuO₂> to demonstrate the applicability of the method. Commercial "<CuO>" of 99.96% purity was equilibrated in oxygen at 1163 K and it gained a weight equivalent to an O/Cu of 0.2, suggesting that it was initially a mixture of <CuO> and <Cu₂O>. After this equilibration, the weight change in a 1.8-g specimen was slight, equivalent to an O/Cu change of 0.0003, over the temperature range 571 to 1166 K. Reductions of 0.4-g samples gave O/Cu values of 1.0004, 1.0002, and 1.0008. A 0.26-g sample of <Y₂BaCuO₅>, which was shown to be single-phased by ceramography, was equilibrated in oxygen at 940 to 1290 K and exhibited no variation in stoichiometry; reduction at 1173 K gave O/M = 1.2533. A sample of "<BaCuO₂>," prepared from <CuO> and <BaCO₃> and known to include some residual carbonate,

demonstrated an O/M variation of about 0.05 from 673 to 1163 K, which is consistent with the literature. Equilibration in oxygen at 1163 K, followed by reduction, gave O/M = 1.027. These results, particularly those for $\langle \text{CuO} \rangle$ and $\langle \text{Y}_2\text{BaCuO}_5 \rangle$, are those expected from the literature and suggest equal validity in application to the "123" compound.

Two reductions of the JB "123" material at 1163 K gave O/6M values of 6.416 and 6.408. Ceramography, which can readily detect less than one volume percent second-phase material, revealed none. These O/M values compare with about 6.388 (Table 1, 890 and 892°C) resulting from the mathematical analysis to be given in Sect. 4. Reduction of the PKG material was also accomplished at 1163 K and gave an O/6M of 6.430. Quantitative ceramography revealed about 0.7% of $\langle \text{CuO} \rangle$, and the effect of this was taken into account.

3.4. O/6M VALUES FOR "123"

The O/6M values for the "123" specimens were calculated from the experimental TGA data. With the weight changes and the initial weight of the specimen, the O/6M change relative to the reference condition of 773 K and $p_{\text{O}_2}^* = 1$ was calculated with a computer program, which also corrected for buoyancy effects and contributions from any second phase. The literature is in reasonable agreement that the O/6M at the latter condition is about 6.92, which we have adjusted to 6.924, as explained later. Thus, the O/6M of the specimen at conditions other than the reference condition is this value plus the experimental change in O/6M. It is believed this method is unique when compared with the literature because all the present experimental O/6M values have the common 773 K reference. Thus, if the 6.924 reference were to be changed in the future, all our other O/6M values would be changed by the same amount.

Late in the course of this investigation, it was found that there was a difference in O/6M results when using a pellet or a similar weight of separated disks cut from the same pellet. [The dimensions are given in Sect. 3.1.] It appeared reasonable that thin disks would give results closest to true equilibrium because oxygen would have to diffuse over a

Table 1. Experimental data for $\langle \text{YBa}_2\text{Cu}_3\text{O}_{7-x} \rangle$

$^{\circ}\text{C}$	$\log_{10} p_0^*$	0/6M	$^{\circ}\text{C}$	$\log_{10} p_0^*$	0/6M
896	0.00	6.3864	548	-3.00	6.3796
500	0.00	6.9251	596	-3.00	6.2785
552	0.00	6.8661	695	-3.00	6.1527
601	0.00	6.7924	794	-3.00	6.0802
649	0.00	6.7036	456	-4.00	6.4557
502	0.00	6.9240	890	0.00	6.3908
697	0.00	6.6182	500	0.00	6.9240
746	0.00	6.5529	447	-1.00	6.9207
797	0.00	6.4917	398	-1.00	6.9650
846	0.00	6.4366	348	-0.99	6.9872
892	0.00	6.3856	319	-0.99	6.9933
304	0.00	6.9971	455	-2.00	6.8058
350	0.00	6.9921	407	-1.99	6.9047
400	0.00	6.9835	307	-1.99	6.9884
450	0.00	6.9629	380	-1.99	6.9433
500	0.00	6.9240	348	-1.99	6.9684
499	-0.99	6.8423	695	-4.01	6.0883
503	-1.01	6.8319	695	-5.00	6.0335
547	-1.01	6.7460	503	-4.00	6.3079
596	-1.01	6.6294	595	-4.00	6.1507
646	-1.01	6.5333	697	-3.99	6.0817
695	-1.01	6.4539	444	-3.00	6.6730
794	-1.01	6.3183	348	-3.01	6.9202
890	-1.01	6.2177	402	-3.00	6.8045
500	0.00	6.9240	309	-3.00	6.9605
500	-1.99	6.6938	405	-3.99	6.6480
548	-1.99	6.5598	547	-5.00	6.1237
597	-1.99	6.4542	309	0.00	6.9991
696	-1.99	6.2841	346	0.00	6.9959
794	-1.99	6.1766	351	0.00	6.9954
889	-1.99	6.1014	401	0.00	6.9851
499	-3.00	6.4983	446	0.00	6.9655
			499	0.00	6.9240

shorter distance. Thus, disks of the JB material were used to generate the 0/6M results given in Table 1. These data are listed in Figs. 3 and 4 in the order they were taken and were obtained in one continuous TGA run of about six weeks duration. The curves in these figures were calculated from the chemical thermodynamic representation to be given in Sect. 4.

The reference 0/6M value of 6.924 was determined with the aid of plots similar to Fig. 4. It can be shown that isobaric data on such a plot become linear as x approaches 0; this results from the Henrian behavior of solutions as the limiting composition is approached. Thus, successive plots were made with different values of the reference 0/6M until the lower-temperature data near $0/6M = 7$ became linear. All of the additional investigations reported below used the reference value of 6.924.

One of our early investigations was a brief comparison of results from the PKG and JB specimens. Low-density pellets of each material were made as described in ref. 1. These were given the standard 1173 and 773 K pretreatment in the TGA in oxygen and then run at 772 to 776 K and 1061 to 1063 K over a range of oxygen partial pressures. The results are shown in Fig. 5 and were essentially the same for both materials. However, comparison of the PKG data in Figs. 1 and 5 illustrates that the present results differ from the earlier work reported by Gallagher et al., particularly at 773 K. This probably results from the difference in experimental techniques. Gallagher et al.¹ used a 1 K/min ramp rate, while the present data were developed isothermally. Also, it can be seen that 1062 K data from the pellets lie above the curves calculated from the data generated from the disks. This can be interpreted to indicate that use of pellets gives a false equilibrium at low temperatures.

The JB pellet was also used in a second TGA system that differed only in that the furnace had a much larger hot zone. The pellet was given the standard 1173 and 773 K pretreatment in the TGA in oxygen, then taken to 973 K. These data are given in Fig. 5 and again indicate that data from the pellet lie above the curve based on data from disks, but that there is no difference resulting from the equipment.

ORNL DWG 88-14948

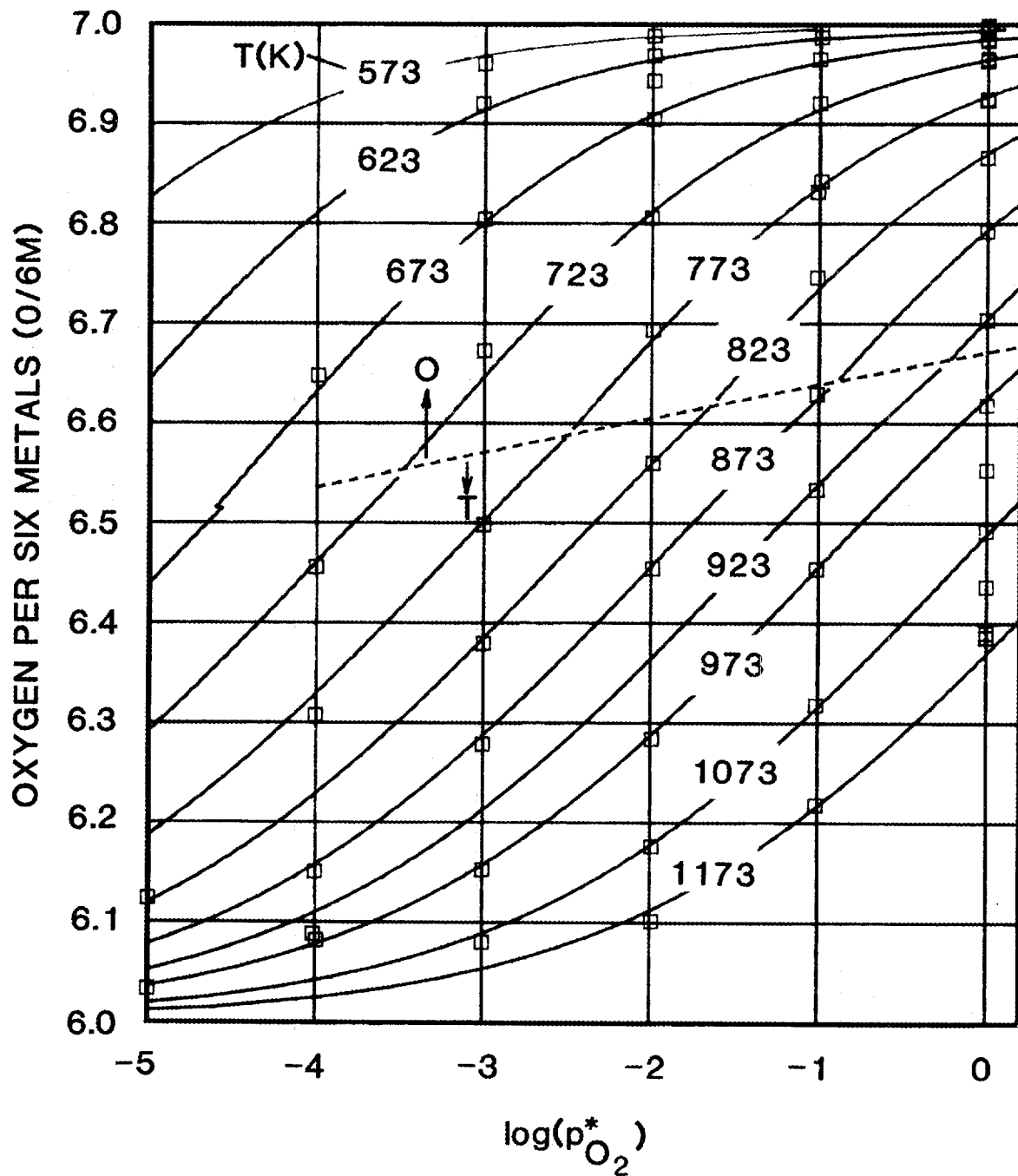


Fig. 4. The data of Table 1 and the fit of the data (lines) calculated from Eq. (9). The orthorhombic-to-tetragonal transition ($0 \leftrightarrow T$, dashed line) is from Specht et al.³

ORNL DWG 88-14947

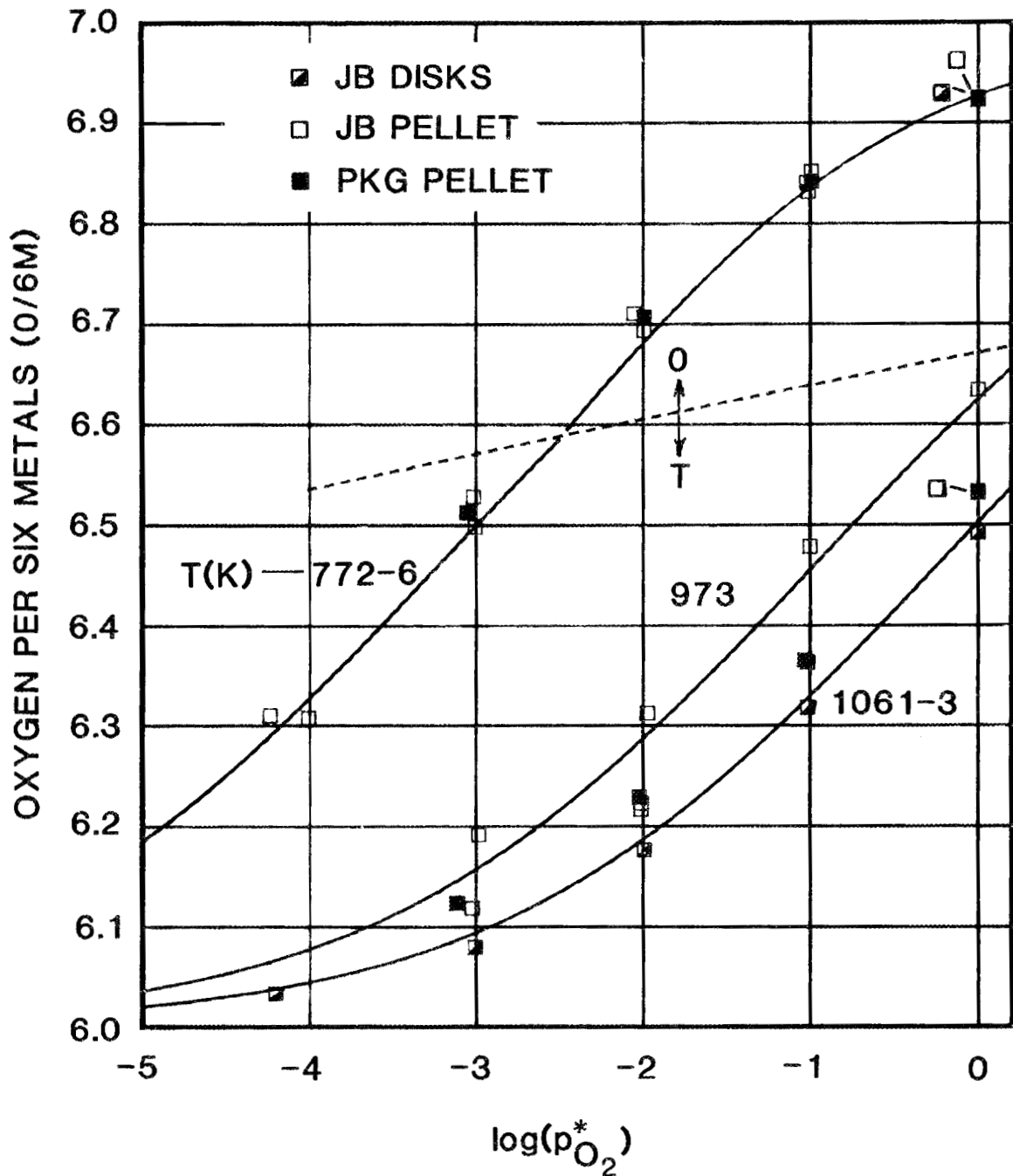


Fig. 5. Comparison of our results from pellets of JB and PKG "123" samples at 772 to 776 K and 1061 to 1063 K, and comparison with the fit of the data (lines) from disks of the JB samples. Also shown at 973 K are the data from a JB pellet treated in a second TGA with a much larger hot zone.

3.5 DECOMPOSITION OF "123"

It was noted during the course of this investigation that the "123" sample would consistently begin to decompose if held at 1173 K and $p_{O_2}^* = 10^{-3}$, whereas it was stable at 1073 K at this pressure. One sample was thus equilibrated at both 1173 K and 773 K in oxygen to establish that the specimen behaved as all others in this study, then decomposed at 1223 K and $p_{O_2}^* = 10^{-4.25}$. It was held there until equilibrium was attained, giving an overall O/6M of 5.21. Subsequent X-ray analysis of the green-colored pellet indicated the phase $\langle Y_2BaCuO_5 \rangle$; in addition, about 10 to 15 lines could not be identified.

3.6 REACTION OF "123" WITH $(CO_2) + (O_2)$

The "123" compound was treated at 1223 K in oxygen, then in an atmosphere of $(O_2-2\% CO_2)$, then $(O_2-70\% CO_2)$. The specimen appeared to equilibrate in both (CO_2) -containing atmospheres. In 2% (CO_2) , the weight gain was equivalent to 60% of the barium oxide component of the "123" being converted to a barium-carbonate-containing compound, while treatment in 70% (CO_2) resulted in complete conversion to a barium carbonate form. X-ray analysis indicated $\langle Y_2BaCuO_5 \rangle$, the orthorhombic form of $\langle BaCO_3 \rangle$, $\langle CuO \rangle$, and a fourth unidentified phase, but not "123." Similar work by Gallagher et al.,¹⁶ detected instead $\langle Y_2Cu_2O_5 \rangle$, $\langle BaCO_3 \rangle$, and $\langle CuO \rangle$.

4. CHEMICAL THERMODYNAMIC REPRESENTATIONS

There are a number of objectives in developing a chemical thermodynamic representation of the nonstoichiometry of the "123" compound. The data indicate that the chemical formula can be written as $\langle YBa_2Cu_3O_{7-x} \rangle$, with $0 < x < 1$. One objective is an accurate representation of the absolute value of the slope, s_1 , of the experimental $\ln(x)-\ln(p_{O_2}^*)$ data as x approaches zero. A plot of these variables is commonly used for non-stoichiometric systems and the slope usually approaches a constant value as x becomes small. At small values of x , the representation to be developed here reduces to the simple expression

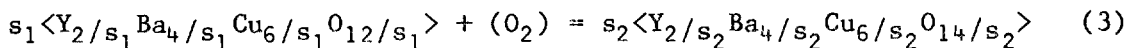
$$\ln(p_{O_2}^*) = a/T + b - s_1 \ln(x) . \quad (1)$$

A second objective is the analogous representation of the $\ln(1-x)-\ln(p_{O_2}^*)$ data as x approaches unity, which will reduce to the simple expression

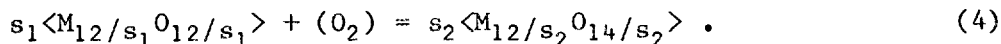
$$\ln(p_{O_2}^*) = c/T + d + s_2 \ln(1-x) . \quad (2)$$

The general approach has been developed by the authors for other nonstoichiometric oxides,^{14,17-22} and will thus be described here in abbreviated fashion.

Several considerations lead to the final representation. The starting point is a chemical equilibrium involving oxygen and, in the present case, two "mass parameters" that are analogous to chemical species in a solid solution, the only difference is that mass parameters may be composed of non-integer numbers of atoms. For the present system, the experimental O/6M data permit one to write two independent mass-balance equations, one for the total mols of oxygen ($7-x$) and one for the total mols of metal (6); and thus the mols of two independent mass parameters may be determined. Since the O/6M values range from 6 to 7, this can be achieved by assuming that one of the mass parameters has an O/6M of 6 and the second mass parameter has an O/6M of 7. These considerations lead to the equilibrium used here,



which was abbreviated to



The left-hand mass parameter has the oxygen-to-metal ratio at $x = 1$, i.e., O/6M = 6, and the right-hand one that for $x = 0$, where O/6M = 7. The mols of each were designated as m_1 and m_2 , respectively, and were calculated from the mass-balance equations for the metals

$$6 = (12/s_1)m_1 + (12/s_2)m_2 \quad (5)$$

and for oxygen

$$7 - x = (12/s_1)m_1 + (14/s_2)m_2 . \quad (6)$$

Upon solving for the mols, one obtains

$$m_1 = 0.5 s_1 x \quad (7)$$

and

$$m_2 = 0.5 s_2 (1-x) . \quad (8)$$

These equations were used to calculate the mol fractions N_1 and N_2 . The equilibrium constant for the equilibrium of Eq. (3) leads to:

$$RT \ln(p_0^*_{O_2}) (J/mol) = \Delta H^\circ_{rxn} - T\Delta S^\circ_{rxn} + s_2 RT \ln(N_2) - s_1 RT \ln(N_1) . \quad (9)$$

This equation was used in a least-squares fit of the experimental data for each crystalline structure of the "123" compound and gave the values of the enthalpy, entropy, and the two slopes. Here, a linear least-squares method was used by iterating over assumed values of s_1 and s_2 and fitting for the enthalpy and entropy terms at a given value of s_1 and s_2 , with the best fit being that with the smallest residuals. The resulting values for the data of Table 1 are given in Table 2 along with the corresponding

Table 2. Fitted values for Eq. (9)

First Author	s_1	s_2	ΔH°_{rxn} (J/mol)	ΔS°_{rxn} (J \cdot mol $^{-1}$ \cdot K $^{-1}$)
Orthorhombic Phase				
This study	2.4	4.0	-171523	-161.34
Gallagher	4.0	3.5	-225300	-213.4
Kishio ^a	5.0	2.0	-290800	-206.5
Specht	2.5	3.0	-160700	-152.8
Strobel	6.0	2.0	-151800	-147.3
Yamaguchi	3.0	2.5	-167000	-166.8
Tetragonal Phase				
This study	4.0	2.8	-163067	-156.28
Gallagher	6.0	3.0	-205300	-196.1
Kishio	4.0	3.0	-185700	-173.9
Specht	6.0	2.0	-146300	-144.6
Strobel	2.5	2.0	-163100	-157.5
Yamaguchi	5.0	2.5	-168100	-170.2

^aData below 500°C were not fitted because the O/6M values approach 6.93 instead of 7.

data for each of the previously published data sets. For the orthorhombic data, the minimum residuals occurred at $s_1 = 2.5$ and $4.0 \leq s_2 \leq 4.3$. The fit at $s_1 = 2.4$ and $s_2 = 4.0$ led to 7% greater residuals; but it was selected because it gave integer subscripts, i.e., M_5O_5 , for the left-hand mass parameter of Eq. (4). For the tetragonal phase, the minimum residuals occurred at $s_1 = 4.8$ and $s_2 = 2.6$. Integer subscripts could be obtained at $s_1 = 4.0$ and $s_2 = 2.8$ with residuals only 10% greater. In addition, this fit gave the best match of the orthorhombic fit to the tetragonal fit at their boundary. Calculations demonstrated, however, that the match could be improved to ± 400 J/mol by adding -720 J/mol to the enthalpy term, which led to the value given in Table 2.

All the data sets were fitted using the data for the orthorhomic-to-tetragonal transition obtained from Specht et al.³ The value of x at the transition, x_{tr} , can be approximated by

$$x_{tr} = [1 + \exp(2.409 - 1636T_{tr}^{-1})]^{-1} \quad (10)$$

in which T_{tr} is the transition temperature in Kelvins. As with most oxide-oxygen equilibria, the oxygen potential for the transition should be nearly linear with temperature, which leads to

$$\log_{10} (p_{O_2, tr}^*) = 11.53 - 10929T_{tr}^{-1}. \quad (11)$$

The partial molal Gibbs free energy expressions for the two mass parameters were also calculated. In general, what is needed first is the value of ΔG_f^0 for $O/6M = 6$ and 7. Morss et al.²³ give $\Delta H_f^0,_{298} = -2675$ kJ/mol for $\langle YBa_2Cu_3O_{6.5} \rangle$ or, from the component oxides, -143 kJ/mol, which is equivalent to a very reasonable -23.8 kJ/(mol metal). The value for ΔS_{298}^0 for the compound has not been reported, even though the required heat capacity has been measured from near 0 K to 298 K. Since these data were given only in relatively inaccurate graphical form, it was assumed here that $S_{f,298}^0$ was the sum of the component oxides, $318.305 \text{ J}\cdot\text{mol}^{-1}\cdot\text{K}^{-1}$. (This compares favorably with the value of $321.16 \text{ J}\cdot\text{mol}^{-1}\cdot\text{K}^{-1}$ from an integration of Cp/T provided by Fisher²⁴ from his review of Cp data²⁵ for specimens estimated to have $6.8 < O/6M < 7.0$.) The resulting $\Delta S_{f,298}$ from the elements is thus $-616.82 \text{ J}\cdot\text{mol}^{-1}\cdot\text{K}^{-1}$. As Kubaschewski and Alcock²⁶ note, a good approximation to the Gibbs free energy of formation at T is

$$\Delta G_f^{\circ}, M_6 O_{6.5} \text{ (J/mol)} = -2675000 + 616.82T . \quad (12)$$

The value of ΔG_f° for $M_{0.7}/_6$ can now be calculated. Green and Leibowitz's²⁷ Eq. (19) demonstrates the technique for integration of oxygen potential over x to obtain the Gibbs free energy of formation per metal atom for a composition having a higher O/M value; this leads to

$$\Delta G_f^{\circ}, M_{0.7}/_6 \text{ (J/mol)} = \Delta G_f^{\circ}, M_{0.5}/_6 + 0.5 RT \int_0^{0.5/6} \ln(p_{O_2}^*) dx . \quad (13)$$

Since the oxygen potential is given by Eq. (9), integration over the limits of x leads to

$$\begin{aligned} \Delta G_f^{\circ}, M_{0.7}/_6 \text{ (J/mol)} &= \Delta G_f^{\circ}, M_{0.5}/_6 + (0.5x)(\Delta H_{rxn}^{\circ} - T \Delta S_{rxn}^{\circ}) \\ &\quad + 0.5 RT (-A \ln A + B \ln B - C \ln C) \end{aligned} \quad (14)$$

in which $A = s_2(1 - x)$, $B = [s_2 + (s_1 - s_2)x]$, $C = s_1x$, and $x = 0.5/6$. For example, with the ΔH_{rxn}° and ΔS_{rxn}° given in Table 2 for the present data for the tetragonal phase, the integration of the oxygen potential term gives

$$\Delta G_f^{\circ}, M_{0.7}/_6 (\text{tet}) \text{ (J/mol)} = \Delta G_f^{\circ}, M_{0.5}/_6 - 6794 + 10.81T . \quad (15)$$

The integration for the orthorhombic phase is

$$\Delta G_f^{\circ}, M_{0.7}/_6 (\text{ortho}) \text{ (J/mol)} = \Delta G_f^{\circ}, M_{0.5}/_6 - 7147 + 9.99T . \quad (16)$$

The partial molal Gibbs free energy, G , can now be derived for each of the two mass parameters. For the orthorhombic phase, the equilibrium is

$$2.4\langle M_5 O_5 \rangle + (O_2) = 4\langle M_3 O_{3.5} \rangle . \quad (17)$$

Equation (16) for 3 mols of metal plus the ideal term give

$$\overline{G}_{M_3 O_{3.5}} (\text{ortho}) \text{ (J/mol)} = -1358888 + 338.39T + RT \ln(N_2) . \quad (18)$$

The enthalpy and entropy terms from this equation, the analogous terms given in Table 2 for the reaction, and the product-reactant difference for the equilibrium of Eq. (17) give

$$\overline{G}_{M_5 O_5} (\text{ortho}) \text{ (J/mol)} = -2193346 + 496.76T + RT \ln(N_1) . \quad (19)$$

Similar considerations for the tetragonal phase, in which the equilibrium is

$$4\langle M_3O_3 \rangle + (O_2) \neq 2.8\langle M_{12}/_2.8O_5 \rangle \quad (20)$$

lead to

$$\bar{G}_{M_{12}/_2.8O_5(tet)}(J/mol) = -1939759 + 486.92T + RT \ln(N_2) \quad (21)$$

and

$$\bar{G}_{M_3O_3(tet)}(J/mol) = -1317064 + 301.78T + RT \ln(N_1). \quad (22)$$

These partials can be used in any thermodynamic calculation involving the orthorhombic or tetragonal phases.

5. GENERAL DISCUSSION

5.1 SUMMARY OF THE x -T- p_0^* DATA

The parameters given in Table 2 for the present study were used to calculate the fitted behavior for comparison with the data, and these results are given in Figs. 3 and 4. Figure 5 illustrates that the present data from the PKG and JB pellets were essentially the same and that the results are not dependent on the origin of the sample. Data from the JB specimen treated in the second TGA system were again essentially the same and demonstrated that the results are not dependent on the equipment.

The present results were compared with the literature data in Figs. 1 and 2. Figure 2 clearly demonstrates the deviation of the data of Kishio et al.² resulting from their limiting O/6M value of 6.93. In addition, the low-pressure data appear too high in O/6M at a given temperature. The data of Yamaguchi et al.⁵ are similar to the present data; if they were displaced about 0.006 O/6M units and 20 K higher, they would agree very closely with the present data. The low-pressure data of Gallagher et al.¹ are apparently displaced too high in O/6M at a given temperature, possibly because equilibrium was not attained with the 1 K/min heating rate. The difficulty in establishing equilibrium at low p_0^* was apparently overcome in the present experiments by (1) grinding the material to <5 μm , (2) use of thin disks, and (3) isothermal treatment that permitted attainment of equilibrium. Times approaching a few days were needed at low pressure, low temperature conditions.

It thus appears that the present data, that of Specht et al.,³ and that of Strobel et al.⁴ are the most consistent over the entire experimental range of variables. The data of Yamaguchi et al.⁵ would also agree with the present data if adjusted 0.006 0/6M units and 20 K higher. The data of Tetenbaum et al.⁹ are also in agreement at $\log(p_{O_2}^*) > -2.8$, but appear to diverge slightly below that condition. The limited data of Takayama-Muromacahi⁷ also appear consistent.

5.2 OXYGEN POTENTIALS IN THE Y-Ba-Cu-O SYSTEM

The oxygen potential plot shown in Fig. 6 is an excellent way to illustrate the complex relationships in this system where the oxygen potential controls the oxidation state of several of the elements. It is unfortunate that there is a general dearth of thermodynamic information on this or analogous systems, but some equilibria can be plotted.

In the metal-oxygen binaries, several equilibria can be shown. The $\langle Cu \rangle - \langle Cu_2O \rangle$,²⁸ $\langle Cu_2O \rangle - \langle CuO \rangle$,²⁸ and $\langle BaO \rangle - \langle BaO_2 \rangle$ ²⁶ equilibria with oxygen are well-known and were plotted on Fig. 6. Both $\langle BaO \rangle$ and $\langle Y_2O_3 \rangle$ are very stable oxides, and the oxide-metal equilibria were below -800 kJ/mol on this plot, with yttria the more stable.²⁸

Consider next the binary oxide systems. Several $\langle BaO \rangle - \langle Y_2O_3 \rangle$ compounds exist, as do $\langle BaCuO_2 \rangle$, $\langle Ba_2CuO_3 \rangle$, and $\langle Y_2Cu_2O_5 \rangle$. For the latter compound, one can estimate thermodynamic data from that for the La-Cu-O system. Chandrasekharaiyah et al.²⁹ report ΔG_f° for $\langle LaCuO_2 \rangle$ and $\langle La_2CuO_4 \rangle$, which leads to the three equilibria shown in Fig. 6 for the La-Cu-O system. In addition, the data lead to

$$\Delta G_{f,ox,La_2Cu_2O_4}^\circ \text{ (J/mol)} = -85900 + 6.53T \quad (23)$$

and

$$\Delta G_{f,ox,La_2CuO_4}^\circ \text{ (J/mol)} = -89540 - 6.69T \quad (24)$$

at 1100 to 1300 K; here $\Delta G_{f,ox}^\circ$ is the Gibbs free energy of formation from the component oxides.²⁸ The compound $\langle La_2Cu_2O_5 \rangle$ has not been reported, but one can calculate an approximate $\Delta G_{f,ox}^\circ$ and use that for the analog

ORNL DWG 88-14952

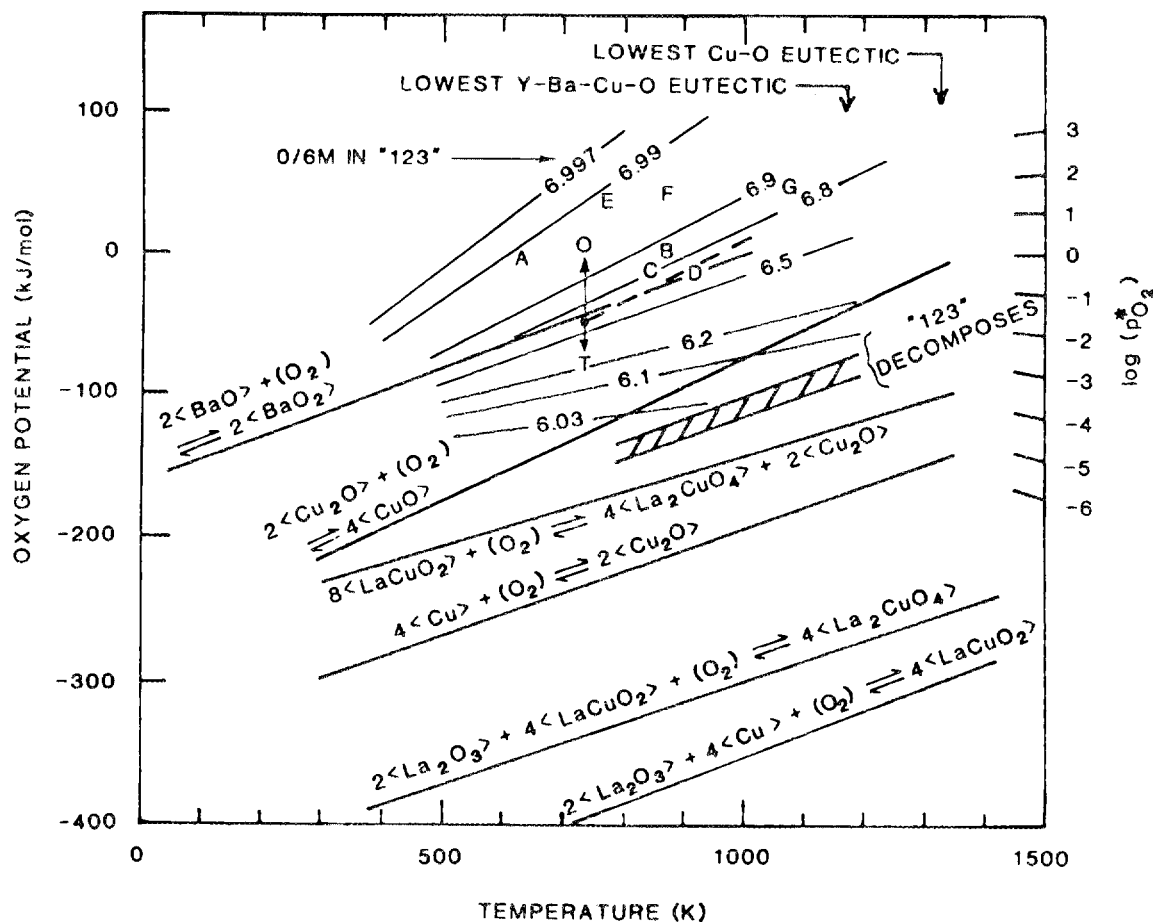
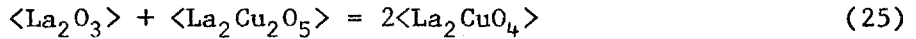
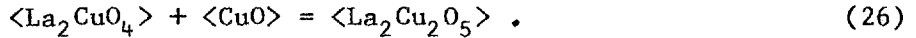


Fig. 6. The oxygen potentials for several equilibria in the Y-Ba-Cu-O and La-Ba-Cu-O systems. Data from ref. 32, as discussed in Sect. 5.2, are as follows. A, condition for $\langle \text{BaCuO}_{2.1} \rangle$; B, $\langle \text{BaCuO}_{2.1} \rangle$ loses oxygen; C, synthesis of $\langle \text{BaCuO}_{2.5} \rangle$; D, $\langle \text{BaCuO}_{2.5} \rangle$ decomposes; E, $\langle \text{BaCuO}_2 \rangle + 0.33(\text{O}_2) \rightleftharpoons \langle \text{BaCuO}_{2.66} \rangle$; F, $\langle \text{BaCuO}_2 \rangle + 0.25(\text{O}_2) \rightleftharpoons \langle \text{BaCuO}_{2.5} \rangle$; G, synthesis of $\langle \text{LaCuO}_3 \rangle$ and $\langle \text{YCuO}_3 \rangle$. The equilibrium $2\langle \text{Y}_2\text{O}_3 \rangle + 2\langle \text{Cu}_2\text{O} \rangle + (\text{O}_2) = 2\langle \text{Y}_2\text{Cu}_2\text{O}_5 \rangle$ is reported³⁰ to be close to that for $2\langle \text{Cu}_2\text{O} \rangle + (\text{O}_2) = 4\langle \text{CuO} \rangle$.

$\langle Y_2 Cu_2 O_5 \rangle$. Two reactions were considered in which two oxide compounds are reacted to form the compound lying between them, namely,



and



The Gibbs free energy for each reaction is <0 , but one can add an increment to each to bring it equal to zero. Upon assuming that the increments are identical for both reactions, one can derive $\Delta G_f^{\circ},_{ox}, La_2 Cu_2 O_5 = 1.5 \Delta G_f^{\circ},_{ox}, La_2 CuO_4$. Upon adding $\Delta G_f^{\circ},_{Y_2 O_3}$ and $2\Delta G_f^{\circ},_{CuO}$ to this, again in the 1000 to 1300 K range,²⁸ one obtains

$$\Delta G_f^{\circ},_{Y_2 Cu_2 O_5} (J/mol) = -2333024 + 441.76T . \quad (27)$$

This estimate permits one to calculate the single equilibrium shown in Fig. 6 for the Y-Cu-O system. A more recent study³⁰ of the oxygen potential of the $\langle Y_2 Cu_2 O_5 \rangle - \langle Y_2 O_3 \rangle - \langle Cu_2 O \rangle$ equilibrium was nearly identical with the oxygen potential of the $\langle Cu_2 O \rangle - \langle CuO \rangle$ equilibrium, and it was not clear which equilibrium was actually studied. If it was the former, then $\langle Y_2 Cu_2 O_5 \rangle$ is much less stable than that given by Eq. (27).

In the absence of thermodynamic information for the $\langle BaO \rangle - \langle CuO \rangle$ and $\langle BaO \rangle - \langle Y_2 O_3 \rangle$ systems, one can only state the rather obvious conclusion that the $\langle BaO \rangle - \langle Y_2 O_3 \rangle$ compounds would be in equilibrium with copper metal at oxygen potentials ranging from slightly below the $\langle Ba \rangle - \langle BaO \rangle$ equilibrium to those approaching the equilibrium shown in Fig. 6 for the Y-Cu-O system. Above this, the oxygen potentials for the several possible equilibria in the $\langle BaO \rangle - \langle Y_2 O_3 \rangle - \langle Cu_2 O \rangle - \langle CuO \rangle$ system cannot be calculated.

Equation (9) was used to calculate the oxygen potentials shown in Fig. 6 for both the orthorhombic and tetragonal "123" phases. Note that the partial molal enthalpy of oxygen, $\bar{\Delta H}(O_2)$, is ΔH_{rxn}° given in Table 1 for Eq. (9). The partial molar entropy of oxygen, $\bar{\Delta S}(O_2)$, at a given 0/6M is $\Delta S_{rxn}^{\circ} - s_2 R \ln(N_2) + s_1 R \ln(N_1)$, as can be seen from Eq. (9). The observation of decomposition presented in Sect. 3.5 is shown as a shaded band at 1100 to 1200 K, and it is a reasonable assumption that this band

can be extended in temperature at approximately the same slope as those shown for the other equilibria. This, in turn, permits one to estimate the minimum O/6M at decomposition of the tetragonal "123" phase. However, these observations are somewhat different from those of Toth et al.,³¹ who reported a similar decomposition in air at 1273 K to give $\langle Y_2BaCuO_5 \rangle$, $\langle CuO \rangle$, and probably $\langle BaCuO_2 \rangle$. It can be seen from Fig. 6 that at 1273 K and ~ 16200 J/mol (i.e., $p_{O_2}^* = 0.21$), the present results indicate that the "123" should still be stable.

Some fragmentary information on the Ba-Cu-O, La-Cu-O, and Y-Cu-O systems is available from the work of Arjomand and Machin.³² Their results are shown in Fig. 6 as points A-G. Some inconsistencies in these results are apparent; "A" and "B" exhibit O/M values less than that for point "C", whereas the opposite would be expected. It is also interesting to note that "D", the decomposition of $\langle BaCuO_{2.5} \rangle$, occurs exactly at the $\langle BaO \rangle$ - $\langle BaO_2 \rangle$ equilibrium, which suggests that the compound is weakly stable relative to the $\langle BaO \rangle$ - $\langle BaO_2 \rangle$ - $\langle CuO \rangle$ components.

The present results, Eq. (9), do not specifically reflect the presence of theoretically predicted phase assemblages. Curtiss et al.³³ predict a two-phase region lying at $6.75 < O/6M < 7.0$, but the temperatures and oxygen pressures for this situation were only schematically described. Our results can be interpreted to indicate that no two-phase region was indicated by the experimental data. Wille et al.³⁴ predict two orthorhombic phases, but the wide two-phase, orthorhombic I-orthorhombic II region was below 500 K, which is lower than our temperature range, and thus not investigated. A predicted second-order transition between the two orthorhombic phases was estimated to occur below ~ 700 K and $\sim 6.55 < O/6M < \sim 6.7$, but was not detected in our rather coarse experimental data. However, the data of Yamaguchi et al.⁵ was taken over smaller increments and may reveal such behavior.

5.3 EQUILIBRIA WITH (CO_2) AND (H_2O)

Several calculated and observed equilibria in the oxide-carbonate and oxide-hydroxide systems are given in Fig. 7. The compilation by Chang and Ahmad³⁵ was a particularly useful source of carbonate thermodynamic data, while a JANAF supplement³⁶ was used for the hydroxide data. This figure illustrates the general interrelationship of the several experimental variables that are relevant during the synthesis of "123" from carbonates, or, conversely, that could lead to conversion of "123" to other phases upon exposure to atmospheres (such as air) that contain (CO_2) and (H_2O). Section 3.6 reported the conversion of "123" in (O_2 - CO_2) atmospheres, and the experimental conditions are plotted on Fig. 7. It is a reasonable assumption that these conditions can be extrapolated to lower temperatures, as shown in Fig. 7. This extrapolation permits one to conclude, e.g., that "123" would, in the absence of kinetic limitations, convert to $\langle \text{BaCO}_3 \rangle$ -containing phases in air below 970 K. Humid air would appear to lead to $\text{Ba}(\text{OH})_2$ -containing phases below about 870 K. Recent work by Gallagher et al.¹⁶ supports this view. Even if kinetic factors prevented complete conversion of the bulk material, the distinct possibility remains that carbonate and hydroxide surface films would form and possibly adversely affect interpretation of fundamental scientific measurements, as well as interfere with electrical connections. The figure also illustrates that, during the hydrogen reduction of "123" to obtain $\langle \text{BaO} \rangle$, $\langle \text{Y}_2\text{O}_3 \rangle$, and $\langle \text{Cu} \rangle$, the temperature needs to be held well above the $\langle \text{BaO} \rangle$ -{ $\text{Ba}(\text{OH})_2$ } equilibrium in order to ensure that barium is present only as $\langle \text{BaO} \rangle$. These conditions are in agreement with the the experimental observations discussed in Sect. 3.3.

We did not consider carbonate-containing solutions because of the lack of thermodynamic data. However, it is well known that the liquid solution of barium oxide and barium carbonate above 1333 K is to be avoided during synthesis of either "123," $\langle \text{BaO} \rangle$, or $\langle \text{BaO}_2 \rangle$ from $\langle \text{BaCO}_3 \rangle$. The work of Roth et al.³⁷ on the Y-Ba-Cu-O- CO_2 phase diagram clearly indicates the possibility of several carbonate-containing solid and liquid solutions as well as eutectics as low as 1173 K.

ORNL DWG 88-14953

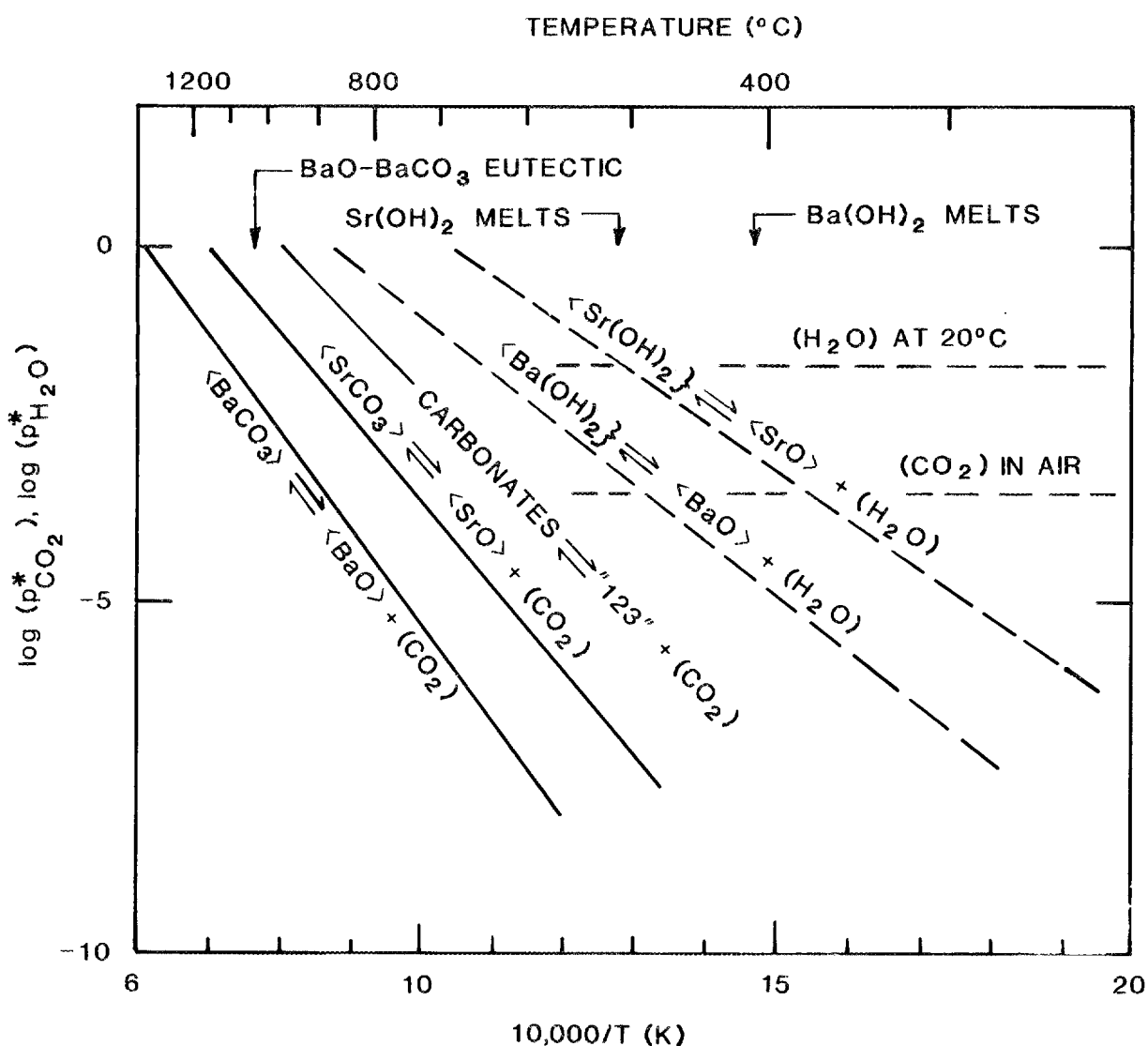


Fig. 7. Dependence of $p_{CO_2}^*$ and $p_{H_2O}^*$ on $10,000/T$ for equilibria in oxide-carbonate and oxide-hydroxide systems.

6. REFERENCES

1. P.K. Gallagher, Adv. Ceram. Matls. 2, 632 (1987).
2. K. Kishio et al., Jpn. J. Appl. Phys. 26, L1228 (1987).
3. E.D. Specht, C.J. Sparks, A.G. Dhere, J. Brynestad, O.B. Cavin, D.M. Kroeger, and H.A. Oye, Phys. Rev. B 37, 7426 (1988).
4. P. Strobel, J.J. Capponi, and M. Marezio, Solid State Comm. 64, 513 (1987).
5. S. Yamaguchi, K. Terabe, A. Saito, S. Yahagi, and Y. Iguchi, Jpn. J. Appl. Phys. 27, L179 (1988).
6. E. Takayama-Muromachi, Y. Uchida, K. Yukino, T. Tanaka, and K. Kato, Jpn. J. Appl. Phys. 26, L665 (1987).
7. E. Takayama-Muromachi, Y. Uchida, M. Ishii, T. Tanaka, and K. Kato, Jpn. J. Appl. Phys. 26, L1156 (1987).
8. T.B. Lindemer and A.L. Sutton, Jr., Review of Nonstoichiometry in $\text{YBa}_2\text{Cu}_3\text{O}_{7-\text{x}}$, ORNL/TM-10827 (1988).
9. M. Tetenbaum, pp. 51-8 in Ceramic Superconductors II, M. F. Yan, ed., The American Ceramic Society, Columbus, Ohio, 1988.
10. J. Marucco, C. Noguera, P. Garoche, and G. Collin, J. Mater. Res. 2, 757 (1987).
11. M. Iwase, H. Iritani, E. Ichise and K. Osamura, Jpn. J. Appl. Phys. 27, L51 (1988).
12. P.K. Gallagher, M.H. O'Bryan, S.R. Sunshine, and D.W. Murphy, Mat. Res. Bull. 22, 995 (1987).
13. S.E. Trolier, S.D. Atkinson, P.A. Fuierer, J.H. Adair, and R.E. Newnham, Am. Ceram. Soc. Bull. 67, 759 (1988).
14. T.B. Lindemer and A.L. Sutton, Jr., J. Am. Ceram. Soc. 71, 553 (1988).
15. P.K. Gallagher, H.M. O'Bryan, and G.S. Grader, submitted for publication.

16. P.K. Gallagher, G.S. Grader, and H.M. O'Bryan, submitted for publication.
17. T.B. Lindemer and T.M. Besmann, J. Nucl. Mater. 130, 473 (1985).
18. T.M. Besmann and T.B. Lindemer, J. Nucl. Mater. 130, 489 (1985).
19. T.M. Besmann and T.B. Lindemer, J. Nucl. Mater. 137, 292 (1986).
20. T.M. Besmann, J. Nucl. Mater. 144, 141 (1987).
21. T.B. Lindemer, CALPHAD 10, 129 (1986).
22. T.B. Lindemer and J. Brynestad, J. Am. Ceram. Soc. 69, 867 (1986).
23. L.R. Morss, D.C. Sonnenberger, and R.J. Thorn, Inorg. Chem. 27, 2106 (1988).
24. R.A. Fisher, Dept. of Chemistry, Univ. of Calif, Berkeley, private communication, October 1988.
25. R.A. Fisher, J.E. Gordon, and N.E. Phillips, J. Supercond., October 1988.
26. O. Kubaschewski and C.B. Alcock, Metall. Thermochem., Fifth ed. (Pergamon Press, New York, 1979).
27. D.W. Green and L. Leibowitz, J. Nucl. Mater. 105, 184 (1982).
28. L.B. Pankratz, "Thermodynamic Properties of the Elements in Oxides," Department of the Interior Bureau of Mines Bulletin 672, (U.S. Government Printing Office, Washington, DC, 1982).
29. M.S. Chandrasekharaiah, M.D. Karkhanavala, and O.M. Sreedharan, High Temp. Science 11, 65 (1979).
30. R. Pankajavalli and O.M. Sreedharan, J. Mater. Sci. Lett. 7, 714 (1988).
31. L.E. Toth et al., Chap. 22 in Chemistry of High Temperature Superconductors, D.L. Nelson, M.S. Whittingham, and T.F. George, eds. (American Chemical Society, Washington, DC, 1987).

32. M. Arjomand and D.J. Machin, J. Chem. Soc. Dalton 1975, 1061 (1975).
33. L.A. Curtiss, T.O. Brun, and D.M. Gruen, Inorg. Chem. 27, 1421 (1988).
34. L.T. Wille, A. Berera, and D. de Fontaine, Phys. Rev. Lett. 60, 1065 (1988).
35. Y.A. Chang and N. Ahmad, Thermodynamic Data on Metal Carbonates and Related Oxides (The Metallurgical Society of AIME, Warrendale, PA, 1982).
36. M.W. Chase, J.L. Curnutt, R.A. McDonald, and A.N. Syverud, J. Phys. Chem. Ref. Data 7(3), 793 (1978).
37. R.S. Roth, C.J. Rawn, F. Beech, J.D. Whitler, and J.O. Anderson, pp. 13-26 in Ceramic Superconductors II, M. F. Yan, ed., The American Ceramic Society, Columbus, Ohio, 1988.

INTERNAL DISTRIBUTION

1.	M. M. Abraham	59.	J. E. Mrochek
2.	B. R. Appleton	60.	B. D. Patton
3.	E. T. Arakawa	61.	S. J. Pennycook
4-8.	E. C. Beahm	62.	D. B. Poker
9-13.	J. T. Bell	63.	M. Rasolt
14.	T. M. Besmann	64.	B. C. Sales
15.	L. A. Boatner	65.	F. M. Scheitlin
16.	W. D. Bond	66.	A. C. Schaffhauser
17.	J. Brynestad	67.	C. D. Scott
18.	J. D. Budai	68-72.	T. C. Scott
19.	B. L. Burks	73.	S. T. Sekula
20.	W. H. Butler	74.	J. Sheffield
21-25.	C. H. Byers	75.	W. D. Siemens
26.	R. S. Carlsmith	76.	C. J. Sparks
27.	Y. K. Chang	77.	E. D. Specht
28.	J. L. Collins	78.	M. G. Stewart
29.	D. K. Christen	79.	J. O. Stiegler
30.	S. J. Dale	80-84.	A. L. Sutton, Jr.
31.	L. B. Dunlap	85.	V. J. Tennery
32.	R. Feenstra	86.	J. R. Thompson
33.	W. A. Fietz	87.	J. Z. Tischler
34.	R. K. Genung	88.	P. J. Walsh
35-39.	M. T. Harris	89.	C. W. White
40-44.	J. R. Hightower	90.	R. K. Williams
45.	E. K. Johnson	91.	R. F. Wood
46.	H. R. Kerchner	92.	F. W. Young, Jr.
47.	H. E. Kim	93.	A. Zucker
48.	D. M. Kroeger	94-95.	Central Research Library
49-53.	T. B. Lindemer	96.	ORNL-Y-12 Technical Library
54.	S. H. Liu	97.	Document Reference Section
55.	D. H. Lowndes	98-99.	Laboratory Records Department
56.	M. S. Lubell	100.	Laboratory Records, ORNL RC
57.	J. McCallum	101.	ORNL Patent Section
58.	H. A. Hook		

EXTERNAL DISTRIBUTION

- 102. R. Barks, Director Industrial Applications Office, Los Alamos National Laboratory, P.O. Box 1663, Los Alamos, NM 87545
- 103. Dr. P. Chaudhari, Vice President Science, International Business Machines (IBM) Corporation, T. J. Watson Research Center, P.O. Box 218, Yorktown Heights, NY 10598
- 104. Dr. G. Y. Chin, Director of Materials Research Laboratory, AT&T Bell Laboratories, R11 1A-164, 600 Mountain Avenue, Murray Hill, NJ 07974

105. Dr. G. Clarke, Manager Program Development, Superconductivity R&D, Westinghouse Electric Corporation, 1310 Beulah Road, Pittsburgh, PA 15235
106. Dr. A. DasGupta, U.S. Department of Energy, Chicago Operations Office, 9800 S. Cass Avenue, Argonne, IL 60439
107. B. Dines, Director of Chemical Physics, AT&T Bell Laboratories, R11 1A-164, 600 Mountain Avenue, Murray Hill, NJ 07974
108. G. Dove, Chairman and CEO, Microelectronics and Computer Corporation, 3500 West Balcones Center Drive, Austin, TX 78759-6509
109. H. Drucker, Associate Director, Argonne National Laboratory, 9700 S. Cass Avenue, Argonne, IL 60439
110. Dr. R. Eaton, III, CE-32, Room 5E-036/FORS, Office of Energy Storage and Distribution, 1000 Independence Avenue, SW, Washington, DC 20585
111. Dr. K. R. Efferson, President, American Magnetics, Inc., P.O. Box 2509, 112 Flint Road, Oak Ridge, TN 37831-2509
112. Dr. J. W. Halloran, Vice President Technology, CPS Superconductor Corporation, 8409 Memorial Drive, Cambridge, MA 02139
113. Dr. J. K. Hulm, Chief Scientist, R&D Center, Westinghouse Electric Corporation, 1310 Beulah Road, Pittsburgh, PA 15235
114. R. A. Jake, Vice President & General Manager, American Magnetics, Inc., P.O. Box 2509, 112 Flint Road, Oak Ridge, TN 37831-2509
115. Dr. K. W. Kline, Director, CE-32, Room 5E-036/FORS, Office of Energy Storage and Distribution, 1000 Independence Avenue, SW, Washington, DC 20585
116. M. Kragie, Analyst, Microelectronics and Computer Corporation, 3500 West Balcones Center Drive, Austin, TX 78759-6509
117. S. Kung, President, Superconductive Products International, 1352 Chatterton Court, Eagan, MN 55123
118. B. Laudies, Director of Materials Chemistry, AT&T Bell Laboratories, R11 1A-164, 600 Mountain Avenue, Murray Hill, NJ 07974
119. J. D. Lloyd, Manager of Advanced Motor Development, Emerson Electric, Motor Division, Emerson Motor Technology Center, 12301 Missouri Bottom Road, Hazelwood, MO 63042-1599
120. Dr. A. P. Malozemoff, Manager, Magnetism and Superconductivity, International Business Machines (IBM) Corporation, T. J. Watson Research Center, P.O. Box 218, Yorktown Heights, NY 10598
121. G. C. Manthey, Chief Energy Technology Branch, Oak Ridge Operations Office, Federal, MS-2067, Oak Ridge, TN 37830
122. D. Murphy, AT&T Bell Laboratories, R11 1A-164, 600 Mountain Ave., Murray Hill, NJ 07974
123. R. Quinn, Director ERDC, Los Alamos National Laboratory, P.O. Box 1663, Los Alamos, NM 87545
124. M. L. Savitz, Director, Allied-Signal Aerospace Company, Garrett Ceramic Components Division, 19800 South Van Ness Avenue, Torrance, CA 90509
125. T. Schlaback, AT&T Bell Laboratories, R11 1A-164, 600 Mountain Avenue, Murray Hill, NJ 07974

126. M. Shafer, International Business Machines (IBM) Corporation, T. J. Watson Research Center, P.O. Box 218, Yorktown Heights, NY 10598
127. M. Stevenson, Deputy Associate Director, Los Alamos National Laboratory, P.O. Box 1663, Los Alamos, NM 87545
128. A. Taub, Manager of Superconducting Materials, General Electric Company, GE Corporate Research and Development, Met Building, Room 263, P.O. Box 8, Schenectady, NY 12301
129. A. Trived, Assistant Manager, Advanced Applications, Allied-Signal Aerospace Company, Garrett AIREsearch, 2525 W. 190th Street, Torrence, CA 90504-6099
130. D. Weeks, Director MCT, Argonne National Laboratory, 9700 S. Cass Ave., Argonne, IL 60439
131. J. Whetten, Associate Director, Los Alamos National Laboratory, P.O. Box 1663, Los Alamos, NM 87545
132. S. Wood, General Manager of Materials Technology Division, Westinghouse Electric Corporation, 1310 Beulah Road, Pittsburgh, PA 15235
133. G. J. Yurek, Vice President of Research, American Superconductor Corporation, 21 Erie Street, Cambridge, MA 02139
134. L. R. Morss, Chemistry Division, Argonne National Laboratory, 9700 S Cass Ave., Argonne, IL 60439
135. M. Tetenbaum, Argonne National Laboratory, 9700 S. Cass Ave., Argonne, IL 60439
136. P. Strobel, Laboratoire de Cristallographic C.N.R.S., Associét à l'U.S.T.M.G., 166X - 38042 Grenoble Cedex, France
137. P. K. Gallagher, AT&T Bell Laboratories, Murray Hill, NJ 07974
138. K. Kishio, Department of Industrial Chemistry, University of Tokyo, Hongo, Bunkyo-ku, Tokyo 113, Japan
139. S. Yamaguchi, Department of Materials Science and Engineering, Nagoya Institute of Technology, Gokiso-cho, Showa-ku, Nagoya 466, Japan
140. E. Takayama, National Institute for Research in Inorganic Materials, 1-1 Namiki, Sakura-mura, Nihari-gun, Ibaraki-ken 305, Japan
141. J. F. Marucco, Laboratoire des Composés non Stoichiometriqués, CNRS, UA 446 Bat. 415, Université de Paris XI, F-91405 Orsay Cedex, France
142. M. Iwase, Department of Metallurgy, Kyoto University, Kyoto 606, Japan
143. R. Escudero, Instituto de Investigaciones en Materiales U.N.A.M., Apartado Postal 70-360, Delegacion Coyoacan, Mexico, D.F. 04510
144. M. Solanki, University of St. Andrews, School of Physical Sciences, North Haugh St., Andrews Fife KY16 9SS, Scotland
145. P. Entel, Theoretische Physik FB 10, Lotharstraße 65, Postfach 10 13 03, D-4100 Duisburg 1, Federal Republic of Germany
146. J. P. Formica, University of Houston, Department of Chemical Engineering, Houston, TX 77204-4792
147. J. J. Lin, Department of Physics, National Taiwan University, Taipei, Taiwan, 10764, Republic of China
148. L. W. Hunter, The Johns Hopkins University, Applied Physics Laboratory, Johns Hopkins Road, Laurel, MD 20707

149. Kai-Yueh Yang, Biomagnetic Technologies, 4174 Sorrento Valley Blvd., P.O. Box 210079, San Diego, CA 92121
150. M. Puri, Department of Chemistry, University of Houston, Houston, TX 77004
151. S. Baliga, Servo Corporation of America, c/s 1490 111 New South Road, Hicksville, NY 11802-9907
152. P. G. Wahlbeck, Wichita State University, Department of Chemistry, Wichita, KS 67208
153. M. W. Barsoum, Department of Materials Engineering, Drexel University, Philadelphia, PA 19104
154. T. B. Tong, Physics Department, Hong Kong Baptist College, 224 Waterloo Road, Kowloon, Hong Kong, Republic of China
155. W. Y. Ching, University of Missouri - Kansas City, Department of Physics, 1110 E. 48th St., Kansas City, MO 64110
156. R. Fisher, Department of Chemistry and Chemical Engineering, University of California, Berkeley, CA 94720
157. Dr. M. Greenblatt, Department of Chemistry, Wright-Rieman Laboratories, Rutgers, The State University, Piscataway, NJ 08854
158. I. Bransky, SYSTRAN Corporation, 4126 Linden Ave., Dayton, OH 45432
159. Amit Goyaz, University of Rochester, Department of Mechanical Engineering, 233 Hopeman Building, University of Rochester, Rochester, NY 14627
160. W. P. Kirk, Texas A&M University, Department of Physics, College Station, TX 77843-4242
161. J. S. Starkovich, TRW Materials Technology, One Space Park, MS 01/2151, Redondo Beach, CA 90278
162. Z. Singh, Fuel Chemistry Division, Bhabha Atomic Research Centre, BARC, Trombay, Bombay-400 085, India
163. R. R. Loh, HiTc Superconco, Inc., P.O. Box 128, 245 N. Main St., Lambertville, NJ 08530
164. D. Cahen, Chemistry Department, Weizmann Institute of Science, P.O.B. 26, Rehovot, Israel 76100
165. L. T. Wille, Department of Physics, Florida Atlantic University, Boca Raton, FL 33431
166. D. L. Myers, Wichita State University, Department of Chemistry, Wichita, KS 67208
167. J. Jorgensen, Argonne National Laboratory, Materials Science Division, Bldg. 223, 9700 S. Cass Ave., Argonne, IL 60439
168. John B. Wachtman, Jr., Department of Ceramics, Rutgers, The State University, P.O. Box 909, Piscataway, NJ 08854
169. Bing Nan Sun, Department of Applied Chemistry, University of Geneva 30, Quai E. Ansermet, CH-1211 Geneva 4, Switzerland
170. John A. Hanigofsky, Georgia Tech Research Institute, Materials Sciences Division, Energy and Materials Sciences Laboratory, Atlanta, GA 30332
171. Andreas Langner, State University of New York at Buffalo, Physics Department, Fronczak Hall, Amherst Campus, Buffalo, NY 14260
172. Donald E. Morris, Lawrence Berkeley Lab, 50-232, Berkeley, CA 94720
173. Raouof Selim, Department of Physics, Christopher Newport College, 50 Shoe Lane, Newport News, VA 23606

174. W. Wong-Ng, U.S. Department of Commerce, National Bureau of Standards, Gaithersburg, MD 20899
175. Amar Nath, Drexel University Chemistry Department, 32nd and Chestnut Sts., Philadelphia, PA 19104
176. C. M. Sung, Materials Science and Engineering, Whitaker Lab, #5, Lehigh University, Bethlehem, PA 18015-3195
177. Doug Morgan, University of Houston, Department of Chemical Engineering, Houston, TX 77204-4792
178. J. Paul Pemsler, Castle Technology Corp., 262 West Cummings Park, Woburn, MA 01801
179. Martha Mecartney, University of Minnesota, Chemical Engineering and Materials Science, 151 Amundson Hall, 421 Washington Ave., SE, Minneapolis, MN 55455
180. Charles A. Parker, Allied-Signal Inc., Engineered Materials Research Center, 50 East Algonquin Road, Box 5016, Des Plains, IL 60017-5016
181. N. A. Gokcen, U.S. Bureau of Mines, Albany, OR 97321
182. R. J. Thorn, Chemistry Division, Argonne National Laboratory, 9700 South Cass Ave., Argonne, IL 60439
183. D. Cordegna, Rochester Institute of Technology, Department of Physics, One Lamb Memorial Drive, P.O. Box 9887, Rochester, NY 14623-0887
184. Iran L. Thomas, Division of Materials Sciences, Office of Basic Energy Sciences, U.S. Department of Energy, Washington, DC 20545
185. R. J. Gottschall, Division of Materials Sciences, Office of Basic Energy Sciences, U.S. Department of Energy, Washington, DC 20545
186. Chalmers Frazer, Division of Materials Sciences, Office of Basic Energy Sciences, U.S. Department of Energy, Washington, DC 20545
187. D. de Fontaine, Department of Materials Sciences and Mineral Engineering, University of California, Berkeley, CA 94720
188. John Hunley, Tennessee Technology University, Box 9693, Cookeville, TN 38505
189. Jacques Gates, 1175 Pelican Drive, Memphis, TN 38109
190. Bernice F. Allen, 2777 Briargrove Dr., #725, Houston, TX 77057
191. Ming Xu, 1134A Mudd Building, Department of Metallurgy and Materials Science, Columbia University, New York, NY 10027
192. Raymond J. Weimer, CORDEC Corporation, 8270-B Cinder Bed Road, Lorton, VA 22079
193. W. Brent Carter, School of Materials Engineering, Georgia Institute of Technology, Atlanta, GA 30332-0245
194. J. S. Faulkner, Department of Physics, Florida Atlantic University, Boca Raton, FL 33433
195. Viren M. Pathare, CPS Superconductor Corp., 840 Memorial Drive, Cambridge, MA 02139
196. E. S. Ramakrishnan, Motorola Inc., Components Division, 4800 Alameda Blvd., N.E., Albuquerque, NM 87113
197. Harry L. Tuller, Crystal Physics and Optical Electronics Lab., Department of Materials Science and Engineering, Massachusetts Institute of Technology, Cambridge, MA 02139
198. R. G. Dorothy, E.I. Du Pont de Nemours & Co., Inc., Experimental Section 304, Wilmington, DE 19898

199. B. C. Johnson, E.I. Du Pont de Nemours & Co., Inc., Experimental Section 304, Wilmington DE 19898
200. D. J. Kountz, E.I. Du Pont de Nemours & Co., Inc., Experimental Section 304, Wilmington DE 19898
201. P. Fischer, Siemens AG Research Center TPH 21, Paul-Gossen-Str. 100, D-8520 Erlangen, Federal Republic of Germany
202. Mu-Yong Choi, Department of Physics, Sung Kyun Kwan University, Suwon 440-746, Korea
203. S. C. Kashyap, Department of Physics, Indian Institute of Technology, Hauz Khas, New Delhi-110016, India
204. Y. Tenbrink, Vacuumschmelze GMBH, Postfach 2253, D-6450 Hanau 1, Federal Republic of Germany
205. N. C. Somi, Bhabha Atomic Research Centre, Metallurgy Division, Trombay, Bombay - 400 085, India
206. M. Acquarone, Universita Degli Studi di Parma, Dipartimento di Fisica, Viale Delle Scienze - 43100 Parma, Italy
207. P. Murugaraj, Max-Planck-Institute fur Festkorperforschung, 7000 Stuttgart 80, Postfach 800665, Federal Republic of Germany
208. Chen Bao-zhu, University of Science and Technology of China, Department of Physics, Anhui Hefei, The People's Republic of China
209. Xe Xiao-guang, University of Science and Technology of China, Department of Physics, Anhui Hefei, The People's Republic of China
210. Klaus Yvon, Laboratoire de Cristallographie aux Rayons X, 24, quai Ernest-Ansermet, CH-1211 Geneve 4, Switzerland
211. J. V. Yakhmi, Government of India, Bhabha Atomic Research Centre, Chemistry Division, Trombay, Bombay - 400 085, India
212. S. Natarajan, Materials Science Research Group, Indian Institute of Technology, Madras - 600 036, India
213. N. Brnjevic, Ruder Boskovic Institute, P.O. Box 1016, 41001 Zagreb, Yugoslavia
214. R. Suryanarayanan, Laboratoirf de Physique, Des Solids, CNRS, 92195 Meudon, France
215. Oscar E. Piro, Departamento de Fisica, Facultad de Ciencias Exactas, Universidad Nacional de La Plata, C.C. 67 (1900) La Plata, Argentina
216. Jeffrey Erxmeyst, Hahn-Meltner-Institut, Berlin GMBH, Glienicker Straße 100, D-1000 Berlin, Federal Republic of Germany
217. S. A. Gavrichkov, L.V. Kirensky Institute of Physics, USSR Academy of Sciences, Siberian Branch, Krasnoyarsk, 660036, USSR
218. E. V. Sampathkumaran, Tata Institute of Fundamental Research, Homi Bhabha Road, Bombay - 400 005, India
219. A. Soloviov, LMF, Joint Institute for Nuclear Research, Head Post Office, P.O. Box 79, Moscow, USSR
220. Zbigniew Bukowski, Instytut Niskich Temperatur I Badan Strukturalnych Pan, 50-950 Wroclaw, Skrytka Pocztowa 937, Poland
221. M. Nunez Regueiro, Centro Atomico Bariloche (C.N.E.A.), 8400 S.C. de Bariloche - R.N., Argentina
222. H. Szymczak, Institute of Physics, Polish Academy of Sciences, Al. Lotnikow 32/46, 02-668 Warszawa, Poland
223. Dr. Rohr, Akademie der Wissenschaften der DDR, Zentralinstitut fur Festkorperphysik und Werkstoffforschung, DDR - 8027 Dresden, German Democratic Republic

- 224. Sanda Adam, IFIN - Fundamental Physics Department, Central Institute of Physics, R-76900, Magurele-Bucharest, P.O. Box MG-6, Romania
- 225. Miguel A. Alario Y Franco, Departmanento de Quimica Inoranica I, Universidad Complutense, Facultad de Ciencias Quimicas, Ciudad Universitaria, 28040 Madrid, Spain
- 226. J. Hauck, Kernforschungsanlage Julich GMBH, Institute IFF, Postfach 1913, D-5170 Julich, Federal Republic of Germany
- 227. Office of Assistant Manager, Energy Research and Development, Oak Ridge Operations Office, Oak Ridge, TN 37831
- 228-237. Office of Scientific and Information Center, Department of Energy, P.O. Box 62, Oak Ridge, TN 37831